Chaotic dynamics of semiconductor lasers with phase-conjugate feedback

George R. Gray
Electrical Engineering Department, University of Utah, Salt Lake City, Utah 84112

David Huang and Govind P. Agrawal
The Institute of Optics, University of Rochester, Rochester, New York 14627
(Received 28 June 1993)

This paper considers the chaotic dynamics of semiconductor lasers in the presence of phase-conjugate feedback (PCF). Bifurcation diagrams are used to explore the chaotic dynamics and show the difference between the conventional feedback and the PCF. In general, semiconductor lasers display richer chaotic dynamics in the case of PCF. Period-doubling, quasiperiodic, and intermittency routes to chaos are observed in numerical simulations performed by using realistic parameter values. For weak values of PCF, the laser can be phase locked to the phase provided by the phase-conjugate mirror, resulting in dramatic narrowing of the laser linewidth. Higher values of feedback result in periodic output, as the laser relaxation oscillations become destabilized. At a critical value of feedback, the laser enters the chaotic regime, resulting in increased low-frequency intensity noise and substantial broadening of the laser line. Finally, the effect of detuning between the solitary-laser frequency and the frequency of the phase-conjugate-mirror pump laser is explored.

PACS number(s): 42.55.Px

I. INTRODUCTION

Semiconductor lasers are known to be extremely sensitive to the optical feedback occurring when a portion of the laser output is fed back into the laser cavity after being reflected from an external reflecting surface. The effect of optical feedback on semiconductor lasers has been extensively studied [1–6]. Quasiperiodic [3], intermittency [4], and period-doubling [5,6] routes to chaos have been observed depending on the operating conditions. Recently, considerable attention has been paid to the case in which optical feedback occurs as a result of reflection from a phase-conjugate mirror (PCM) [7–17]. Such feedback is referred to as phase-conjugate feedback (PCF) and differs considerably from conventional optical feedback (COF) since the phase of the returned light is reversed during reflection. Although the stability of semiconductor lasers in the presence of PCF has been studied [15–17], the chaotic dynamics of such lasers have not yet been explored in detail.

In this paper, bifurcation diagrams are used to identify the chaotic and nonchaotic regions and show the difference between the PCF and COF. In general, semiconductor lasers display richer chaotic dynamics in the case of PCF. Period-doubling, quasiperiodic, and intermittency routes to chaos are observed in numerical simulations performed by using realistic parameter values. The noise characteristics in the presence of PCF are studied by adding the Langevin noise terms representing the effect of spontaneous emission to the rate equations and solving them numerically. For weak values of PCF, the laser can be phase locked to the phase provided by the PCM, resulting in dramatic narrowing of the laser linewidth. This narrowing is shown in both the frequency noise spectrum (FNS) and the laser line shape. As the PCF is increased, all the spectra show that the relaxation oscillations, which are shifted by 30% from the solitary-laser value, become undamped. With further increase in the PCF, the laser output becomes chaotic at a critical value of PCF. In the chaotic regime, the intensity noise at low frequencies (below 100 MHz) is considerably enhanced and the relaxation-oscillation peak becomes much broader. In addition, the spectral line shape develops strong satellite peaks at multiples of the relaxation-oscillation frequency, which merge together to result in a broad line shape indicative of coherence collapse. We assume for simplicity that the PCF is provided by a perfect phase-conjugate mirror (PCM) that responds almost instantaneously. Four-wave mixing inside a fast nonlinear medium (response time <1 ps) pumped by a narrow-linewidth laser can provide a PCM whose performance approaches the ideal PCM assumed here. We consider both degenerate and nearly degenerate four-wave mixing.

The paper is organized as follows. In Sec. II the rate equations for a semiconductor laser in the presence of PCF are given and the various parameters are described. These rate equations are solved numerically in Sec. III, and the chaotic dynamics are investigated through the use of bifurcation diagrams. The effect of chaos on the relative intensity noise (RIN), the frequency noise, and the spectral line shape is shown in Sec. IV. In Sec. V we consider the case of a PCM employing nearly degenerate four-wave mixing such that a detuning exists between the PCM pump laser and the semiconductor laser under study. A summary of the basic results and conclusions are presented in Sec. VI.

II. RATE EQUATIONS WITH PCF

The dynamical behavior of semiconductor lasers is generally modeled by a set of rate equations by assuming

that the dipole relaxation time (T_2 in the terminology of two-level systems) is short enough that the gain medium is able to respond almost instantaneously to the changes in the optical field. The effect of PCF on the semiconductor laser depends on the type of PCM and is different for PCM's based on photorefraction and four-wave mixing. Here we consider the case of a four-wave-mixing PCM pumped by a laser whose frequency is close to the operating frequency of the semiconductor laser. In the presence of PCF, these equations can be written as (assuming single-mode operation) [15–17]

$$\frac{dE}{dt}=\left[-i\frac{1}{2}\alpha G_N(N-N_{\rm sol})+\frac{1}{2}\left[G-\frac{1}{\tau_p}\right]\right]E(t)+F_E(t)$$
$$+\kappa E^*(t-\tau)\exp\left[2i\Delta\omega\left[t-\frac{\tau}{2}\right]+i\phi_{\rm PCM}\right], \quad (1)$$

$$\frac{dN}{dt}=\frac{I}{q}-\frac{N}{\tau_e}-G|E(t)|^2+F_N(t), \quad (2)$$

where $E(t)$ is the slowly varying complex amplitude of the intracavity optical field, $\Delta\omega=\omega_0-\omega_p$ is the frequency mismatch between the solitary semiconductor laser and the laser used to pump the PCM, τ_p is the photon lifetime, α is the linewidth enhancement factor, N is the electron population, $N_{\rm sol}$ is its steady-state value in the absence of feedback, I is the injection current, q is the magnitude of the electron charge, τ_e is the electron lifetime, and G is the net rate of stimulated emission assumed to vary linearly with the electron population as

$$G=G_N(N-N_0)(1-\varepsilon P). \quad (3)$$

In Eq. (3), N_0 is the transparency value of N and the parameter G_N is related to the derivative of the optical gain with respect to the carrier density; P is the photon number, and ε is the nonlinear-gain parameter. The Langevin noise sources $F_E(t)$ and $F_N(t)$ represent the noise introduced by spontaneous emission and the shot noise due to carrier generation and recombination, respectively.

The last term in Eq. (1) is due to PCF and contains four parameters κ, τ, $\Delta\omega$, and $\phi_{\rm PCM}$. The feedback rate κ and the round trip time τ are given by

$$\kappa=\frac{(1-R_m)}{\tau_L}\left[\frac{\eta_c R_{\rm PCM}}{R_m}\right]^{1/2}, \quad \tau=\frac{2L_{\rm ext}}{c}, \quad (4)$$

where η_c is the coupling efficiency, R_m is the laser facet reflectivity, τ_L is the round trip time in the laser cavity, $R_{\rm PCM}$ is the reflectivity of the PCM, and $L_{\rm ext}$ is the spacing between the laser and the PCM. The parameter $\phi_{\rm PCM}$ accounts for a constant phase shift occurring at the PCM. The round trip phase shift $2\Delta\omega(t-\tau/2)$ in Eq. (1) results from the phase-conjugate nature of the feedback and is nonzero only because of the frequency mismatch; when $\Delta\omega=0$, any accumulated one-way phase shift gets canceled exactly during the return trip. Note that the PCM is assumed to respond instantaneously in Eq. (1). If the PCM response is slower than the round trip time τ, κ would become time dependent. This case can be studied by adding a third equation that governs the PCM dynamics to the set of Eqs. (1) and (2).

The steady-state solution of Eqs. (1) and (2) has been investigated [15–17]. The results show that for weak feedback—the exact value of which depends on the detuning—the laser frequency locks to that of the PCM and the phase of the laser is pinned to a value determined by the phase of the PCM according to

$$2\phi+\phi_{\rm PCM}+\tan^{-1}(\alpha')=2m\pi, \quad (5)$$

where ϕ is the (slowly varying) steady-state phase, m is an integer, and $\alpha'=\alpha/(1+\varepsilon P_s)$ [18], with $P_s=(G_N\tau_e)^{-1}$ representing a saturation photon number. In contrast, for normal feedback the steady-state phase remains arbitrary, as in the case for no feedback. It was previously predicted from linearized theory [17] that the pinning or locking of the laser phase would lead to a laser line shape consisting of a spike at low frequencies (since the long-time behavior of the phase is locked), superimposed on a broader pedestal (since spontaneous emission still causes the short-time behavior of the phase to wander). This is confirmed in this paper by simulation of the full nonlinear equations, as shown in Sec. III.

Another difference between PCF and COF in the weak-feedback regime concerns the dependence on feedback phase $\omega_0\tau$. For COF the laser is very sensitive to the precise value of the feedback phase. The threshold gain is either increased or decreased, the laser frequency can be shifted either positively or negatively, and the laser line is either broadened or narrowed depending on the exact value of feedback phase. In contrast, for a single-mode laser with PCF and zero detuning, the feedback phase does not enter into the equations, making the results independent of feedback phase. Specifically, the change in gain induced by feedback can be written as

$$\Delta G=\frac{-2\kappa\cos(2\phi+\phi_{\rm PCM})}{1+\varepsilon P_s}$$
$$=\frac{-2\kappa\alpha'}{\alpha\sqrt{1+\alpha'^2}}$$
$$=\frac{-2\kappa}{(1+\varepsilon P_s)\sqrt{1+\alpha'^2}}, \quad (6)$$

where use was made of Eq. (5). The change in gain, therefore, depends only on κ and various material parameters. In the same manner, Eqs. (5) and (6) can be used to write the frequency shift in the presence of weak PCF as

$$\Delta\omega=\tfrac{1}{2}\alpha\Delta G-\kappa\sin(2\phi+\phi_{\rm PCM})=\tfrac{1}{2}\alpha\Delta G+\frac{\kappa\alpha'}{\sqrt{1+\alpha'^2}}=0. \quad (7)$$

Therefore, when the laser is in this phase-locking regime, there is no induced frequency shift for the degenerate (no detuning) PCM regardless of the feedback phase or the phase incurred at the PCM. These results stand in stark contrast with the case of COF, for which phase locking can only occur for a single value of feedback phase, namely $\omega_0\tau=-\tan^{-1}(\alpha')$.

However, in a manner similar to COF—when the PCF exceeds a critical value—relaxation oscillations become

undamped and the laser output becomes periodic. With further increase in the PCF, the laser enters the chaotic regime. In this paper we explore this chaotic region. To investigate the chaotic dynamics, we have solved Eqs. (1) and (2) numerically by using a fourth-order Runge-Kutta algorithm. The parameter values used correspond to a typical index-guided Ga-Al-As semiconductor laser likely to be used in optical recording systems. These values are listed in Table I and result in a threshold current of 61 mA and a slope efficiency of about 0.5 mW/mA. We expect qualitatively similar conclusions for comparable laser parameters. The chaotic dynamics are most sensitive to the external cavity length, the linewidth-enhancement factor, and the nonlinear-gain parameter; the dependence on these parameters is investigated below. Most of the simulations are presented for a solitary-laser power of 1.6 mW, which is a typical value used for reading data from an optical disk in optical data recording systems.

III. BIFURCATION DIAGRAMS

For quantifying the chaotic dynamics occurring in single-mode lasers, the use of bifurcation diagrams and Poincaré sections is well established [3]. The bifurcation diagram, in particular, is a powerful tool for investigating the laser behavior with optical feedback, since the diagram shows at a glance for which strengths of feedback the laser operates stably, periodically or chaotically. We begin by showing a series of bifurcation diagrams to point out the differences between PCF and COF. Figures 1(a) and 1(b) show bifurcation diagrams for an external cavity length of $L_{\text{ext}}=10$ cm and linewidth-enhancement factor $\alpha=3$ for the cases of PCF and COF, respectively. For the case of COF, the feedback phase was chosen to be zero; different feedback phases do not significantly change the conclusions drawn here. The feedback phase for PCF is irrelevant since it gets canceled in the roundtrip. Also, the phase shift obtained at the PCM, ϕ_{PCM}, although affecting the phase-locked state [see Eq. (5)], does not change the bifurcation diagrams. The bifurcation diagrams were obtained by generating a time series for each feedback level and then noting the carrier number N when the laser power crossed the solitary-laser value, P_{sol}. A trajectory of at least 160 ns was discarded to allow for transients to die out. Generally speaking, a single crossing in the bifurcation diagram implies a periodic output whereas multiple crossings indicate period doublings, quasiperiodicity, or chaos. The random noise terms have been neglected in making these diagrams, so that we may separate the deterministic effects from stochastic effects. The parameter $\kappa\tau$ is varied over a wide range ($\kappa\tau=0-5$) covering R_{PCM} in the range from 0% to 5%.

A comparison of Figs. 1(a) and 1(b) reveals both the similarities and the differences between PCF and COF. In both cases, the steady state (corresponding to the blank regions without any dots) becomes unstable at a critical value of κ, and the laser output becomes periodic, presumably as a result of the undamping of relaxation oscillations. However, several differences exist between the bifurcation diagrams for PCF and COF. First, although in both cases chaos is interrupted by regions of nonchaotic output, for PCF the output does not become completely stable (cw) as it does in the COF case. That is, in the COF diagram [Fig. 1(b)], following the first chaos region, the laser reverts to a fixed-point solution (no intersection in the bifurcation diagram) for $\kappa\tau>2.2$; in the PCF diagram, on the other hand, a chaotic solution is always followed by a periodic limit-cycle solution (a single intersection in the bifurcation diagram). The second obvious difference between the two diagrams is that the chaotic regions for PCF are qualitatively more complicated than those for COF. That is, the bifurcation diagram for PCF is more completely filled than that for COF. Somewhat surprisingly, the correlation dimensions calculated from time series show little difference between PCF and COF. For example, the dimensions were calculated for feedback levels corresponding to the middle of the first chaotic attractor in Fig. 1: $\kappa\tau=1.1$ for PCF [Fig. 1(a)] and $\kappa\tau=1.5$ for COF [Fig. 1(b)]. The PCF dimension was 2.52, compared to 2.48 for the COF case. Such a trend

TABLE I. Typical parameter values used in numerical simulations for a 780-nm Ga-Al-As semiconductor laser

Parameter	Symbol	Value
Laser cavity length	L	350 μm
Solitary laser roundtrip time	τ_L	9.3 ps
Linewidth enhancement factor	α	3
Laser facet reflectivities	R_1, R_2	0.9,0.12
Photon lifetime (using internal loss of 65 cm^{-1})	τ_p	1.4 ps
External cavity length	L_{ext}	10 cm
External cavity roundtrip time	τ	0.67 ns
Carrier recombination time	τ_e	2 ns
Gain coefficient	G_N	$1.19\times10^3\,\text{s}^{-1}$
Transparency carrier number	N_0	1.64×10^8
Nonlinear-gain parameter	ε	3.57×10^{-8}
Bias current	I_B	65.1 mA
Average output power	P_{out}	1.6 mW
Coupling efficiency	η_c	2%
Feedback phase	$\omega\tau$	see text

was found for other $\kappa\tau$ values, but the difference is probably not statistically significant. The program used to calculate the dimensions was based on standard techniques [20] and the program was tested on the Henon map, for which the correlation dimension is well known. The comparison of dimensions is complicated by the fact that the chaotic attractors occur for different values of $\kappa\tau$ for COF and PCF. In general, when comparing two chaotic regions of the same type of feedback, the one for the larger $\kappa\tau$ value will tend to have the larger correlation dimension.

A third difference which is not apparent from the bifurcation diagram involves the frequency of the first periodic solution. The frequency is best seen by calculating the intensity-noise spectrum and, for the COF case, the frequency is very close to the solitary laser relaxation-oscillation frequency ν_R (773 MHz for the parameters in Table I). This provides strong evidence that the relaxation oscillations have become undamped. However, in the case of PCF, the intensity-noise spectrum reveals that the period of oscillation is 500 MHz, which is much smaller than ν_R and is exactly 1/3 of the external cavity roundtrip frequency $1/\tau$. If this frequency is still to be interpreted as the relaxation-oscillation frequency, then it seems to have been pulled away from the solitary-laser value by almost 30%.

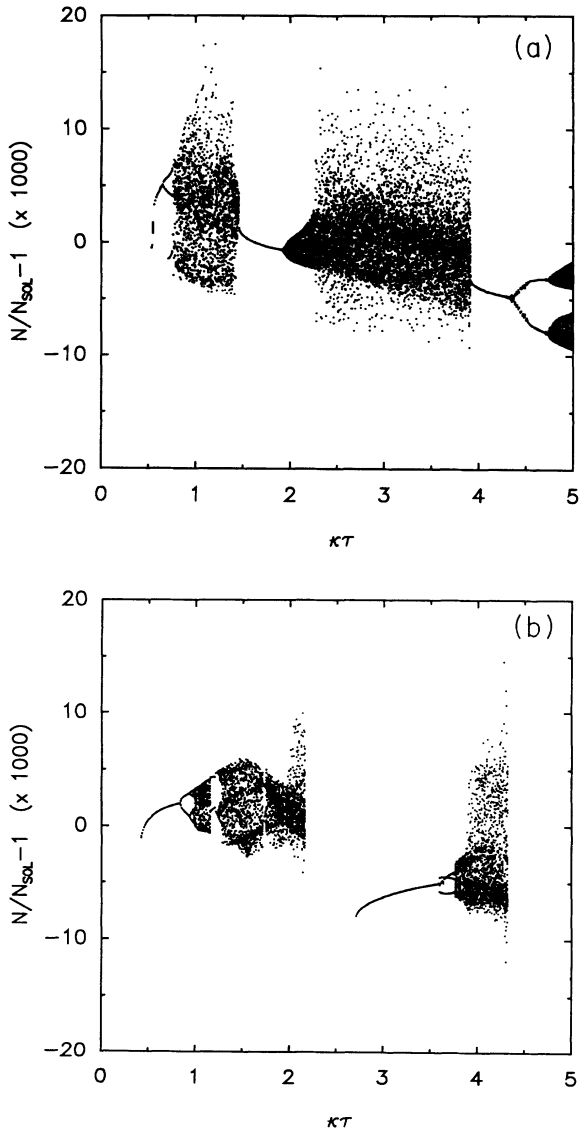

FIG. 1. Bifurcation diagrams in the cases of (a) PCF and (b) COF for $L_{ext}=10$ cm and $\alpha=3$. Other parameter values are shown in Table I. In the absence of feedback ($\kappa\tau=0$) the laser operates stably with 1.6 mW output power.

The origin of these differences between the two types of feedback is related to the methods by which the stable solutions become unstable. In either case, a standard small-signal analysis of the laser-rate equations for photon number, phase, and carrier number leads to eigenvalue equations whose solutions determine the steady-state stability. In the case of relatively weak feedback, this set of eigenvalue equations reduces to a cubic polynomial with three roots (see Refs. [16,17]), a complex-conjugate pair, and one real root. When no feedback is present, the real root is zero and the imaginary and real parts of the complex-conjugate pair represent respectively the frequency and the damping rate of the relaxation oscillations. When feedback is present, the laser can go unstable in two ways: (i) when the real part of the complex-conjugate pair becomes positive (corresponding to undamping of relaxation oscillations) and (ii) when the real root becomes positive. In the case of COF, when the real root becomes positive it implies an external cavity mode jump to a stable mode. For PCF in a single-mode laser and zero detuning, there are no external cavity modes; once this real root becomes positive, the laser remains unstable (i.e., the laser remains in a non-cw state). This is seen in the bifurcation diagrams for PCF, because there are no stable regions after the first route to chaos. Also, the real root becomes positive at lower values of feedback than for COF. This may partially explain the fact that the chaotic dynamics tends to be more complex for the case of PCF. It must be pointed out that only in the weak-feedback limit ($\kappa\tau \ll 1$) can the roots from the eigenvalue analysis be found analytically, thereby yielding an expression for the frequency of relaxation oscillations in the presence of feedback [1].

The chaotic dynamics is quite sensitive to the external cavity length L_{ext}. Figures 2(a) and 2(b) show bifurcation diagrams under conditions identical to those of Fig. 1, except that L_{ext} has been reduced to 5 cm. In the case of COF, the laser becomes much less sensitive to the feedback since the cw state remains stable over a wide range of $\kappa\tau$ except over narrow windows of chaos seen in Fig. 2(b). In contrast, the cw state is never stable for PCF once it becomes unstable at a relatively small value of $\kappa\tau$. The chaotic regions are much wider in the case of PCF and are interrupted by periodic or quasiperiodic states. For higher values of feedback, the chaos develops following a quasiperiodic route to chaos in both cases. The differences become less apparent in the long external cavity limit ($\tau > 1/\nu_R$). Figures 3(a) and 3(b) show bifurcation diagrams for $L_{ext}=30$ cm. Both cases become unstable at similar feedback levels, although they follow different routes to chaos. A characteristic of the long external cavity limit [19] is that once the laser becomes

chaotic it is unlikely to return to a stable state at higher feedback levels, in contrast to shorter external cavities [see Fig. 2(b), for example]. The other apparent difference for $L_{ext}=30$ cm is that for PCF, overlapping attractors are present in the bifurcation diagram at higher feedback levels ($\kappa\tau>3$). Specifically, beyond $\kappa\tau=4$ both chaotic and quasiperiodic attractors are simultaneously present in the bifurcation diagram. Which attractor the laser chooses to follow is very sensitive to initial conditions. Overlapping attractors have been observed for COF as well [3]. In general, the chaos occurs over a large range of feedback levels for longer external cavities for both PCF and COF.

The chaotic dynamics depend on many other laser parameters. Two parameters which control chaos most are the linewidth-enhancement factor α and the nonlinear-gain parameter ε. In general, the semiconductor laser is much more susceptible to chaos for higher values of α and lower values of ε. The dependence of chaos on ε is easily understood if we note that the damping rate of relaxation oscillations increases linearly with ε. Thus, relaxation oscillations become undamped at smaller feedback levels for lower values of ε. The dependence of chaos on α can be understood by noting that larger values of α imply larger phase changes associated with the feedback. Indeed, chaos is found to disappear for $\alpha=0$. For a given value of α, the laser becomes more chaotic in the case of PCF compared with COF. As an example, Figs. 4(a) and 4(b) compare the bifurcation diagrams for PCF and COF when $\alpha=1.5$ and $L_{ext}=10$ cm. Whereas chaos has almost disappeared in the case of COF, it dominates the dynamics in the case of PCF. This difference is attributed to the fact that PCF tends to lock the laser phase (which changes because of α) and thus can

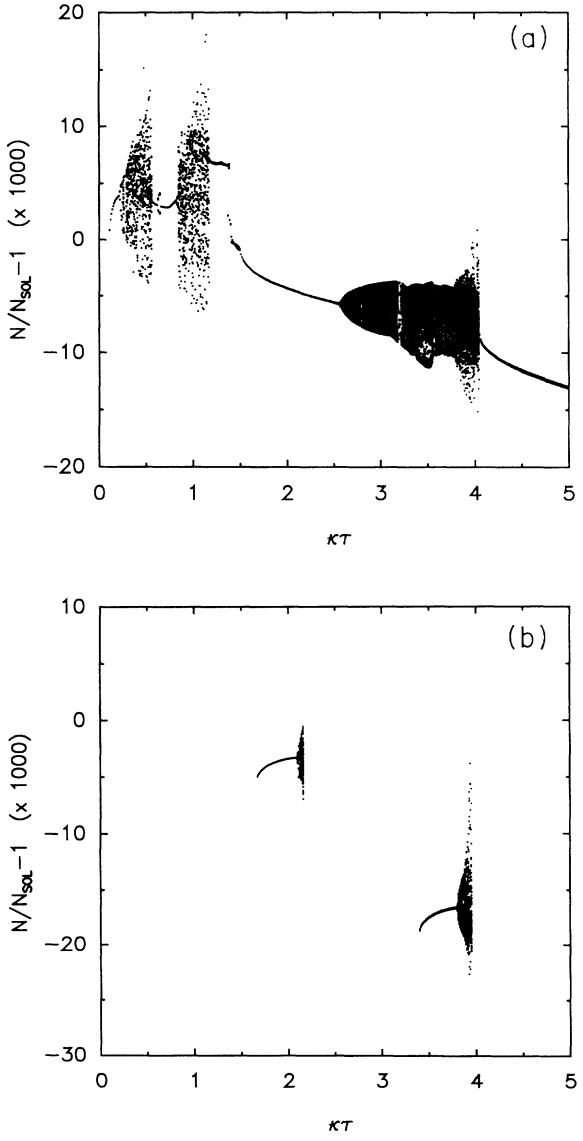

FIG. 2. Same as in Fig. 1 except that the external-cavity length L_{ext} has been reduced from 10 to 5 cm. The semiconductor laser is stable over a wide range of $\kappa\tau$ in the case of COF.

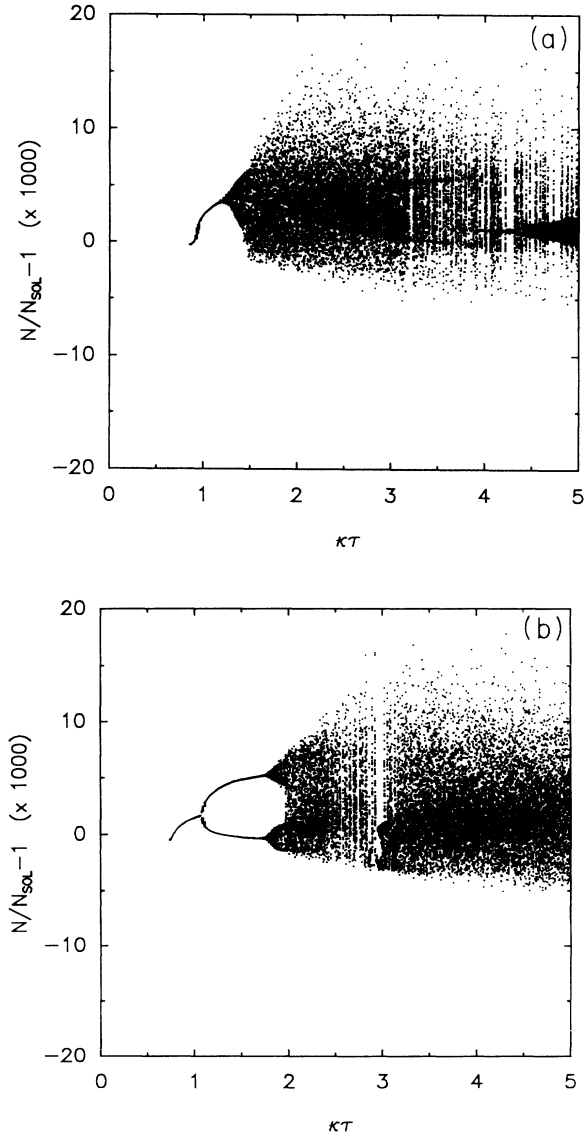

FIG. 3. Same as in Fig. 1 except that the external-cavity length L_{ext} has been increased to 30 cm. There are fewer differences between PCF and COF for longer external cavities.

destabilize the laser even for relatively small values of α.

The bifurcation diagram for PCF and $\alpha=1.5$, Fig. 4(a), looks somewhat unusual because chaos apparently begins without some type of "route" to chaos. The explanation for this strange appearance is as follows. As $\kappa\tau$ is increased to about $\kappa\tau=1$, the laser output is a stable fixed-point solution; however, as $\kappa\tau$ increases beyond 1, this fixed-point solution becomes periodic as the relaxation oscillations become undamped, although the laser takes longer and longer to settle down to this periodic steady state. Indeed, for $\kappa\tau=1.2$, the laser takes more than 300 ns to settle down to a periodic solution. The reason this periodic solution doesn't appear as a point in Fig. 4(a) is because the amplitude of the periodic solution is too small to intersect the $P=P_{\text{sol}}$ plane, which is the way the bifurcation diagram is constructed. In the $\alpha=3$ case (Figs. 1–3), the amplitude of the periodic state becomes larger and larger until the solution bifurcates toward chaos. In contrast, for $\alpha=1.5$, chaos is reached by the intermittency route. Figure 5 shows the laser power vs time for $\kappa\tau=1.3$, demonstrating that the laser exhibits intermittent bursts of chaotic output; [note that time scale in Fig. 5(a) is more than 1 μs]. Such intermittent bursts are known to be a source of low-frequency fluctuations in lasers with COF. Figure 5(b) shows a blown up version of Fig. 5(a) in order to show the high-frequency oscillations. Such intermittent bursts were not seen with these laser parameters for any of the other cases considered in this paper. Since different types of intermittent behavior have been identified, the analysis of which type is present in this case will be the subject of a future paper.

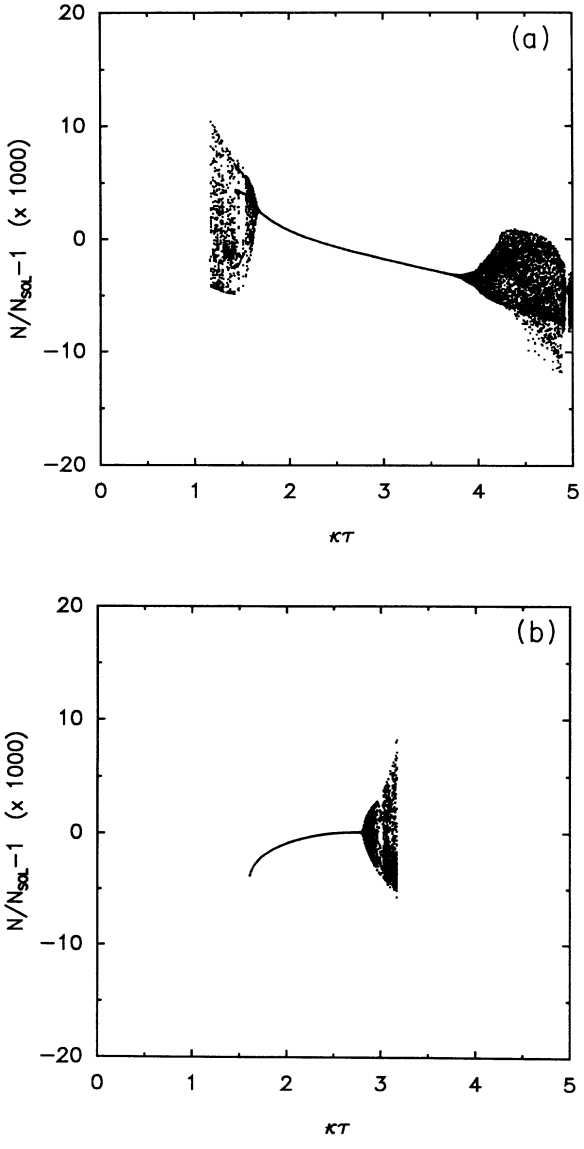

FIG. 4. Same as in Fig. 1 except that the linewidth enhancement factor α has been reduced from 3 to 1.5. The chaotic regions becomes sparser for smaller values of α in the cases of both PCF and COF. For PCF, the laser experiences an intermittency route to chaos (see Fig. 5).

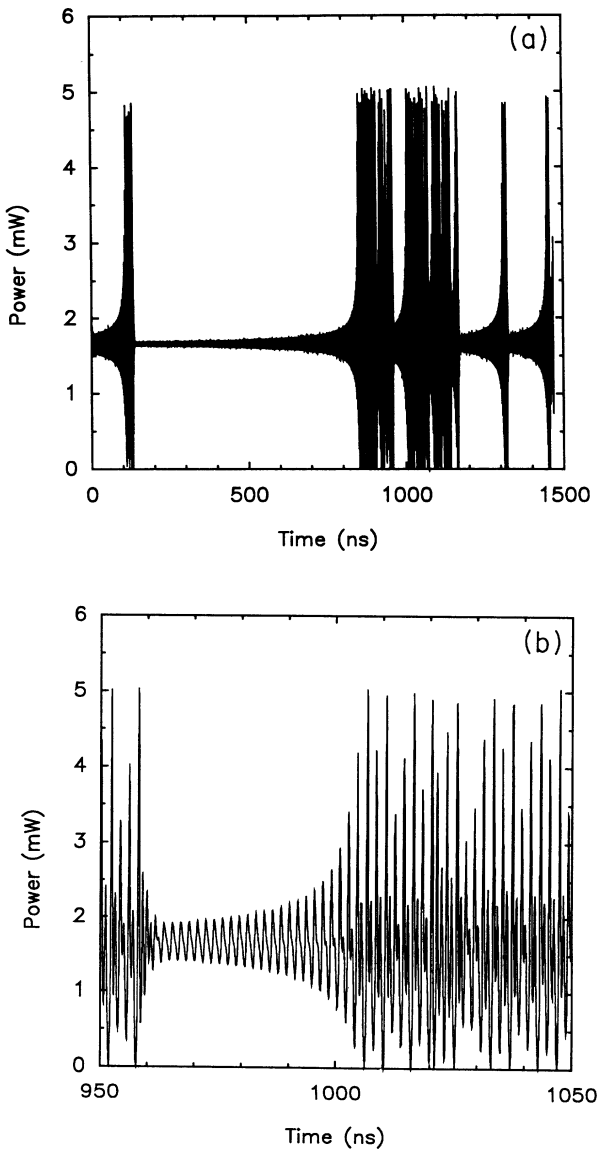

FIG. 5. (a) Long-time trajectory for PCF at $\kappa\tau=1.3$ showing that the laser power undergoes intermittent bursts of chaotic output. (b) Blowup of a small region of (a) showing details of temporal evolution.

IV. EFFECT OF PCF ON NOISE SPECTRA

From a practical standpoint, one is often interested in the effects of optical feedback on the intensity and phase noise of semiconductor lasers. It is well known [2,17] that at small feedback levels such that the laser's steady state remains stable, both PCF and COF can reduce the low-frequency intensity and frequency noise, a feature that can be used for practical applications. However, when the feedback level increases and destabilizes the steady state, one expects the laser noise to increase. This section discusses the effects of periodic and chaotic dynamics on the laser noise by considering the relative-intensity noise (RIN), frequency-noise spectrum (FNS), and the spectral line shape defined as

$$S_I(\nu)=\frac{1}{\bar{P}^2}\int_{-\infty}^{\infty}\langle\delta P(t)\delta P(t+t')\rangle\exp(-2\pi i\nu t')dt' , \tag{8}$$

$$S_F(\nu)=2\pi\int_{-\infty}^{\infty}\langle\delta\nu(t)\delta\nu(t+t')\rangle\exp(-2\pi i\nu t')dt' , \tag{9}$$

$$S(\nu)=\int_{-\infty}^{\infty}\langle E^*(t+t')E(t)\rangle\exp(-2\pi i\nu t')dt' , \tag{10}$$

where $E=\sqrt{P}\exp(-i\phi)$, $\delta P=P-\bar{P}$ represents a power fluctuation from the average value $\bar{P}$, and $\delta\nu(t)$ is the frequency fluctuation. The spontaneous-emission-induced stochastic fluctuations are included through the Langevin noise source $F_E(t)$ in Eq. (1) and are assumed to be δ-function correlated (in the Markoffian approximation); i.e.,

$$\langle F_E(t)F_E^*(t')\rangle=R_{sp}\delta(t-t') , \tag{11}$$

where the rate of spontaneous emission $R_{sp}=n_{sp}/\tau_p$, and n_{sp} is the population inversion factor. We choose $n_{sp}=1.8$ in the following simulations. The Langevin noise source $F_N(t)$ in Eq. (2) was ignored as its effect on the laser noise was found to be negligible [1]. All of the spectra represent an average over at least five trajectories of length $\sim$300 ns in order to improve numerical accuracy; this yields a frequency resolution of about 3 MHz. The parameter values used are given in Table I; in particular, $L_{ext}=10$ cm and $\alpha=3$, as in Fig. 1(a).

Figure 6 compares the RIN spectra (after performing a five-point running average for smoothing) for $\kappa\tau=0$ (no PCF; short-dashed curve), $\kappa\tau=0.6$ (periodic dynamics; long-dashed curve) and $\kappa\tau=1$ (chaotic dynamics; solid curve). In the absence of PCF, the solitary laser has a relatively low RIN (~-130 dB/Hz) at low frequencies (<100 MHz) and exhibits the well-known peak at the relaxation-oscillation frequency (at about 800 MHz for the parameters used in the simulation). When the PCF is large enough to destabilize the steady state but not large enough to induce chaos, the periodic dynamics of the laser manifests through a much stronger relaxation-oscillation peak in the RIN spectrum, indicating that the laser output is periodic at the relaxation-oscillation frequency. Note that the relaxation-oscillation frequency is shifted to 500 MHz from the solitary value, as discussed above. The second harmonic of this frequency is also apparent in the RIN spectrum. Even the low-frequency RIN is raised by about 5 dB for this value of feedback. For $\kappa\tau=1$ the laser output exhibits chaos, as manifested in the RIN spectrum by two features—the low-frequency RIN is increased by 10 dB over the solitary-laser value, and the relaxation-oscillation peak has become very broad. The RIN increase is well known in the case of COF [2,6], and is a consequence of the broadband deterministic noise induced by the chaotic dynamics.

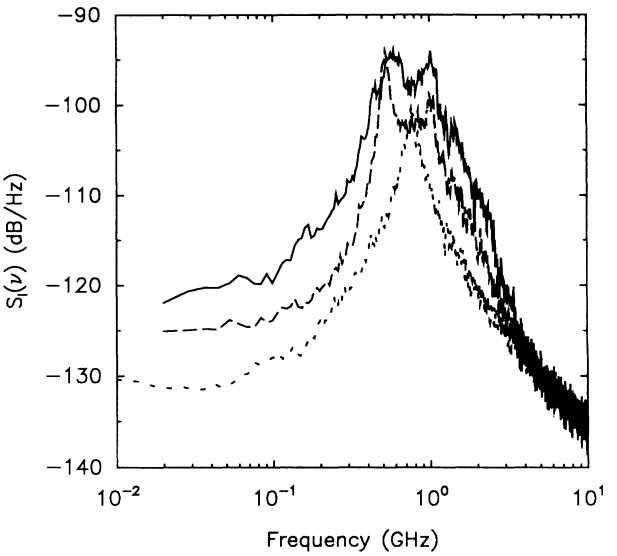

FIG. 6. RIN spectra for $\kappa\tau=0$ (- - - -), 0.6 (— — —), and 1.0 (——) under conditions identical to those of Fig. 1(a). The low-frequency RIN is enhanced by 10 dB in the chaotic regime.

The FNS (also smoothed using a five-point running average), under the conditions identical to those of Fig. 6, is shown in Fig. 7. In the absence of PCF (short-dashed curve), the FNS agrees well at all frequencies with the an-

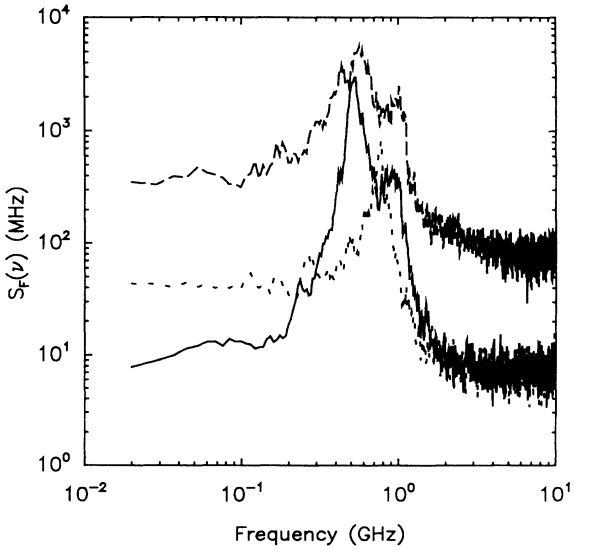

FIG. 7. Frequency-noise spectra for $\kappa\tau=0$ (- - - -), 0.5 (——), and 1.0 (— — —). For $\kappa\tau=0.5$ the low-frequency part of the FNS is reduced due to the phase-locking nature of the PCF. The low-frequency FNS is greatly increased when the laser is in the chaotic regime ($\kappa\tau=1$).

alytic expression obtained from linearized theory. Indeed, when intensity fluctuations can be neglected, the low-frequency value of the FNS can be shown to equal the laser linewidth (with our normalization) [1]. For the parameters used in the simulation, the solitary-laser linewidth is approximately 40 MHz. Because of the coupling between amplitude and phase in semiconductor lasers, the FNS shows the relaxation-oscillation peak also present in the RIN. For a feedback of $\kappa\tau=0.5$ (long-dashed curve) this peak is enhanced by an order of magnitude and shifted to 500 MHz, as discussed above. The low-frequency part of the FNS, on the contrary, is reduced by about a factor of 5 for this value of feedback. By examination of Fig. 1(a), we see that $\kappa\tau=0.5$ should correspond to the frequency-locked state, and the apparent reduction in laser linewidth is evidence that the laser phase is also being locked. For $\kappa\tau=1$ (solid curve) the laser output is chaotic and the apparent linewidth approaches the opposite limit; i.e., the low-frequency part of the FNS is increased by an order of magnitude over the solitary-laser value. The FNS also shows an increased and broadened relaxation-oscillation peak as well as enhanced high-frequency noise.

The effects of PCF on the laser linewidth is most naturally examined through the laser line shape, which is shown in Fig. 8 for four values of feedback. The line shapes are plotted on identical vertical scales but shifted vertically for clarity (no running average was performed for the line shapes). For $\kappa\tau=0$ [no PCF; curve (*a*)], the line shape exhibits well-known features of a solitary laser [1,2], namely a narrow, central, Lorentzian peak, accompanied by much weaker sidebands due to relaxation oscillations. For $\kappa\tau=0.5$ [phase-locked state; curve (*b*)], the central peak has dramatically narrowed due to the phase-locking nature of the PCF. This line shape, consisting of a central spike riding on top of a broad pedestal, was predicted from linearized theory in Ref. [17]. The weak oscillation at 500 MHz shows up as shifted but enhanced sidebands. For $\kappa\tau=0.6$ [periodic state; curve (*c*)], the sidebands continue to increase in magnitude and are nearly as high as the central peak, which is not as narrow as that of curve (*b*). This implies that the laser is undergoing a transition from the phase-locked state to the periodic state. Finally, curve (*d*) corresponds to the chaotic state and we see why such a state is also termed "coherence collapse." The line shape is extremely broadband since the central and satellite peaks have become so broad that they merge together. With the notable exception of the phase-locked, narrow linewidth state, these qualitative features are similar to those seen in the case of conventional optical feedback.

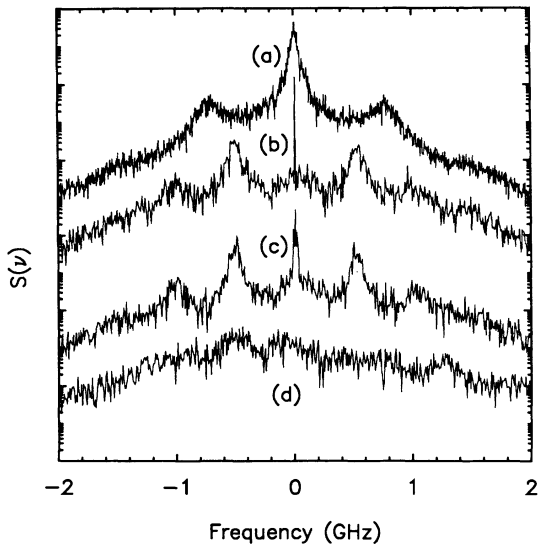

FIG. 8. Spectral line shapes for $\kappa\tau=0$ [(a); no PCF], 0.5 [(b); phase-locked state], 0.6 [(c); periodic state] and 1.0 [(d); chaotic state]. All spectra are plotted on identical vertical scales which are shifted vertically for clarity. Note the dramatic line narrowing of the phase-locked state (b) and the undamped relaxation oscillations of the periodic state (c). In the chaotic regime the multiple sidebands merge to yield a broad spectrum indicative of coherence collapse.

V. EFFECT OF PUMP-PROBE DETUNING

In this section we no longer assume that the PCM is produced by degenerate four-wave mixing but instead allow for a frequency mismatch between the laser used to pump the PCM and the solitary semiconductor laser frequency. This generalization is expected to make the PCF case even more complex relative to COF. Indeed, with a detuning present, the PCF case can be considered a combination of feedback (which provides the delay) and injection locking (which provides the detuning). We begin with a relatively small value of detuning $\Delta\omega/2\pi=100$ MHz. Figure 9 shows the corresponding bifurcation diagram by using the same parameters as in Fig. 1. A comparison of Fig. 9 and Fig. 1(a) reveals minor but important differences which arise because of the detuning. Most importantly, the diagram shows that for small values of feedback ($\kappa\tau<0.14$), the laser output is period-

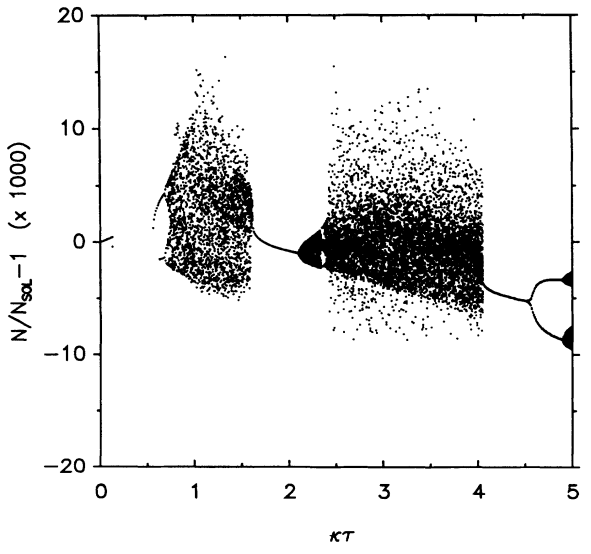

FIG. 9. Bifurcation diagram for PCF and 100 MHz detuning. Other parameters same as in Fig. 1. Note the presence of a periodic output for very small values of $\kappa\tau$ [compare with Fig. 1(a)] because of four-wave mixing.

ic. This is shown clearly in Fig. 10, which shows the laser power vs time for four different values of feedback. For $\kappa\tau < 0.05$ [Fig. 10(a)] the laser output consists of weak periodic oscillations at a frequency of 200 MHz, which is twice the detuning $\Delta\omega/2\pi$. The origin of these oscillations lies in the feedback-induced four-wave mixing and can be understood as follows. Since the frequency of the feedback light differs from the laser frequency by $2\Delta\omega$, the mutual interference between the two waves leads to carrier-density modulation at $2\Delta\omega$, which in turn generates periodic output and the four-wave-mixing sidebands separated by $2\Delta\omega$. Interestingly, as $\kappa\tau$ increases above 0.06, the modulation frequency decreases below 200 MHz, as shown in Fig. 10(b)–10(d). Beyond a critical value of feedback ($\kappa\tau > 0.13$), the periodic state abruptly yields to a fixed-point solution, and the laser operates continuously (cw operation). The high-frequency oscillations seen in (c) and (d) correspond to the laser's relaxation oscillations. The interpretation of Fig. 10 is as follows. For weak feedback the laser frequency is close to its solitary-laser value but oscillates at twice the detuning. However, as feedback increases, the feedback-induced frequency shift reduces the effective detuning $\Delta\omega$, and the four-wave-mixing sidebands move closer. Eventually, the detuning becomes small enough that it falls inside the injection-locking bandwidth, forcing the laser to injection lock to the pump frequency of the PCM. This is confirmation of the behavior described by Tartwijk, van der Linden, and Lenstra [16] who have examined the stability properties of PCF with nonzero detuning.

A case for larger detuning of 1 GHz is shown in Fig. 11. Although the high-feedback portion of the diagram is similar to Fig. 1(a), the low-feedback region is significantly different. For this large detuning the laser

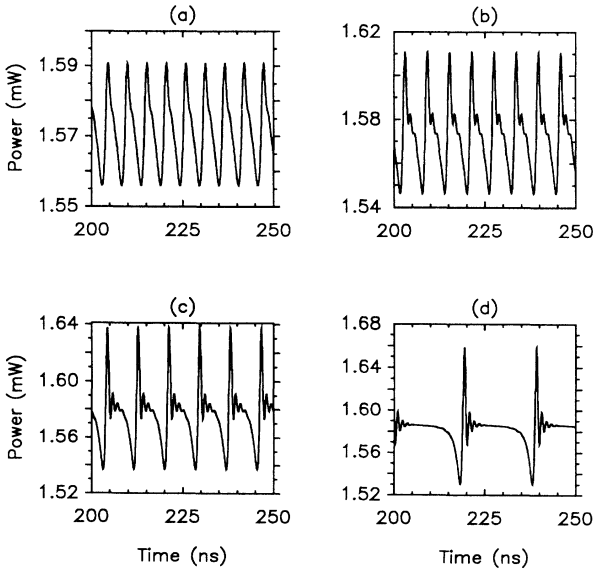

FIG. 10. Power vs time trajectories in the weak feedback regime of Fig. 9 corresponding to four-wave mixing. Trajectories (a)–(d) correspond to $\kappa\tau = 0.05$, 0.08, 0.11, and 0.13, respectively. The modulation frequency decreases from its initial value of 200 MHz as $\kappa\tau$ increases.

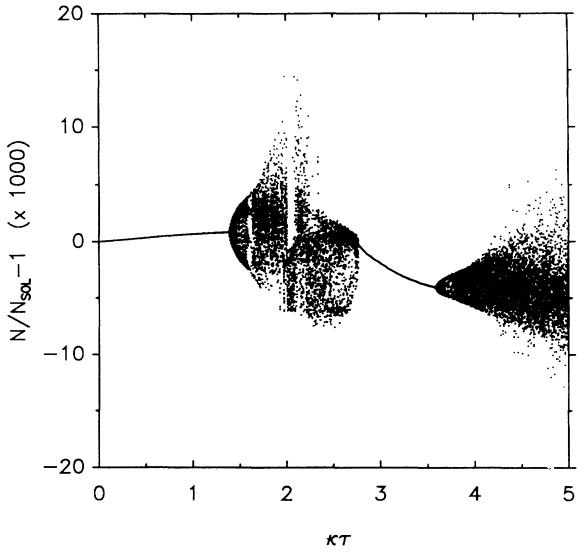

FIG. 11. Bifurcation diagram similar to Fig. 9 but for a large detuning of 1 GHz. In contrast to Fig. 9, the periodic solution due to the detuning does not give way to the cw operation before becoming chaotic.

power oscillates at twice the detuning (2 GHz) for $\kappa\tau < 1.2$. Beyond this value of feedback, the oscillation frequency increases to about 2.2 GHz until, by $\kappa\tau = 1.4$, a second frequency of 600 MHz appears in the noise spectrum and the laser enters directly into the chaotic region, following a quasiperiodic route to chaos, without experiencing injection locking. This behavior can be understood by noting that the feedback-induced frequency shift is too small to reduce the effective detuning so that it lies within the injection-locking bandwidth. This large-detuning behavior also agrees with the predictions of Ref. [16].

VI. CONCLUSIONS

This paper considers the chaotic dynamics of semiconductor lasers in the presence of phase-conjugate feedback (PCF). By using the single-mode, rate-equation formalism, it is shown that the output of semiconductor lasers becomes chaotic when the amount of PCF exceeds a critical value. Bifurcation diagrams are used to explore the chaotic dynamics and show the difference between the conventional feedback and the PCF. In general, semiconductor lasers display richer chaotic dynamics in the case of PCF. Period-doubling, quasiperiodic and intermittency routes to chaos are observed in numerical simulations performed by using realistic parameter values. The noise characteristics in the presence of PCF are studied by adding the Langevin noise terms (representing the effect of spontaneous emission) to the rate equations and solving them numerically. For weak values of PCF, the laser can be phase locked to the phase provided by the PCM, resulting in dramatic narrowing of the laser linewidth. The line narrowing, unlike the case of COF, is not dependent on the feedback phase. This narrowing is shown in both the frequency-noise spectrum (FNS) and the laser line shape. As the PCF is increased, all the spectra show that

the relaxation oscillations, which are shifted by 30% from the solitary-laser value, become undamped. In the chaotic regime, the intensity noise at low frequencies (below 100 MHz) is considerably enhanced and the spectral line shape broadens considerably, indicative of coherence collapse. The inclusion of detuning $\Delta\omega$ between the solitary-laser frequency and the frequency of the PCM pump laser shows that the laser exhibits four-wave mixing at low feedback such that the output is periodic at $2\Delta\omega$. For small detuning, the laser can injection lock to the pump-laser frequency and operate cw before entering the chaotic regime. For large detuning, injection locking does not occur, and the laser enters the chaotic state directly from the periodic state. In both cases the chaotic dynamics remains largely unaffected by the detuning.

ACKNOWLEDGMENTS

This work is supported by the U.S. Army Research Office and the New York State Foundation of Science and Technology. G.R.G. acknowledges the support from the University Research Committee.

[1] G. P. Agrawal and N. K. Dutta, *Semiconductor Lasers*, 2nd ed. (Van Nostrand Reinhold, New York, 1993), Chap. 6 and references cited therein.
[2] K. Petermann, *Laser Diode Modulation and Noise* (Kluwer Academic, Dordrecht, Netherlands, 1991), Chap. 9.
[3] J. Mork, B. Tromborg, and J. Mark, IEEE J. Quantum Electron. **28**, 93 (1992); A. Ritter and H. Haug, J. Opt. Soc. Am. B **10**, 130 (1993); **10**, 145 (1993).
[4] J. Sacher, W. Elsasser, and E. O. Gobel, Phys. Rev. Lett. **63**, 2224 (1989).
[5] J. Ye, H. Li, and J. G. McInerney, Phys. Rev. A **47**, 2249 (1993).
[6] G. R. Gray, A. T. Ryan, G. P. Agrawal, and E. C. Gage, Opt. Eng. **32**, 729 (1993).
[7] K. Vahala, K. Kyuma, A. Yariv, S. Kwonk, M. Cronin-Golomb, and K. Y. Lau, Appl. Phys. Lett. **49**, 1563 (1986).
[8] M. Cronin-Golomb and A. Yariv, Opt. Lett. **11**, 455 (1986); M. Cronin-Golomb, A. Yariv, and I. Ury, Appl. Phys. Lett. **48**, 1240 (1986).
[9] R. R. Stephens, R. C. Lind, and C. R. Giuliano, Appl. Phys. Lett. **50**, 647 (1987); J. O. White, G. C. Valley, and R. A. Macfarlane, *ibid.* **50**, 880 (1987).
[10] A. M. C. Smout and R. W. Eason, Opt. Lett. **12**, 498 (1987); M. D. Ewbank, Opt. Lett. **13**, 47 (1988).
[11] M. Segev, S. Weiss, and B. Fischer, Appl. Phys. Lett. **50**, 1397 (1987); M. Segev, Y. Ophir, B. Fischer, and G. Eisenstein, *ibid.* **57**, 2523 (1990).
[12] M. Ohtsu, I. Koshishi, and Y. Teramachi, Jpn. J. Appl. Phys. **29**, L2060 (1990); N. Cyr, M. Breton, M. Tetu, and S. Theriault, Opt. Lett. **16**, 1298 (1991).
[13] B. H. W. Hendriks, M. A. M. de Jong, and G. Nienhuis, Opt. Commun. **77**, 435 (1990).
[14] Y. Champagne, N. McCarthy, and R. Tremblay, IEEE J. Quantum Electron. **25**, 595 (1989); N. McCarthy and D. Gay, Opt. Lett. **16**, 1006 (1991); N. McCarthy, S. Maihot, and J. F. Cormier, Opt. Commun. **88**, 403 (1992).
[15] G. P. Agrawal and J. T. Klaus, Opt. Lett. **16**, 1325 (1991).
[16] G. H. M. van Tartwijk, H. J. C. van der Linden, and D. Lenstra, Opt. Lett. **17**, 1590 (1992).
[17] G. P. Agrawal and G. R. Gray, Phys. Rev. A **46**, 5890 (1992).
[18] A. Ritter and H. Haug, J. Opt. Soc. Am. B **10**, 130 (1993).
[19] A. T. Ryan, G. P. Agrawal, G. R. Gray, and E. C. Gage, IEEE J. Quantum Electron (to be published).
[20] P. Grassberger and I. Procaccia, Phys. Rev. Lett. **50**, 346 (1983).

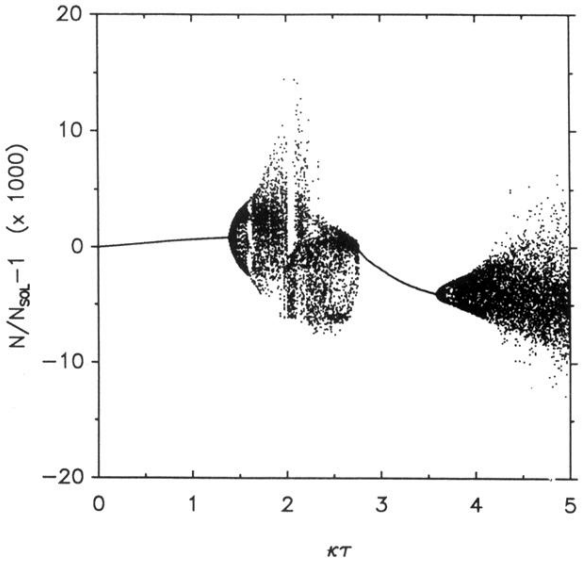

FIG. 11. Bifurcation diagram similar to Fig. 9 but for a large detuning of 1 GHz. In contrast to Fig. 9, the periodic solution due to the detuning does not give way to the cw operation before becoming chaotic.

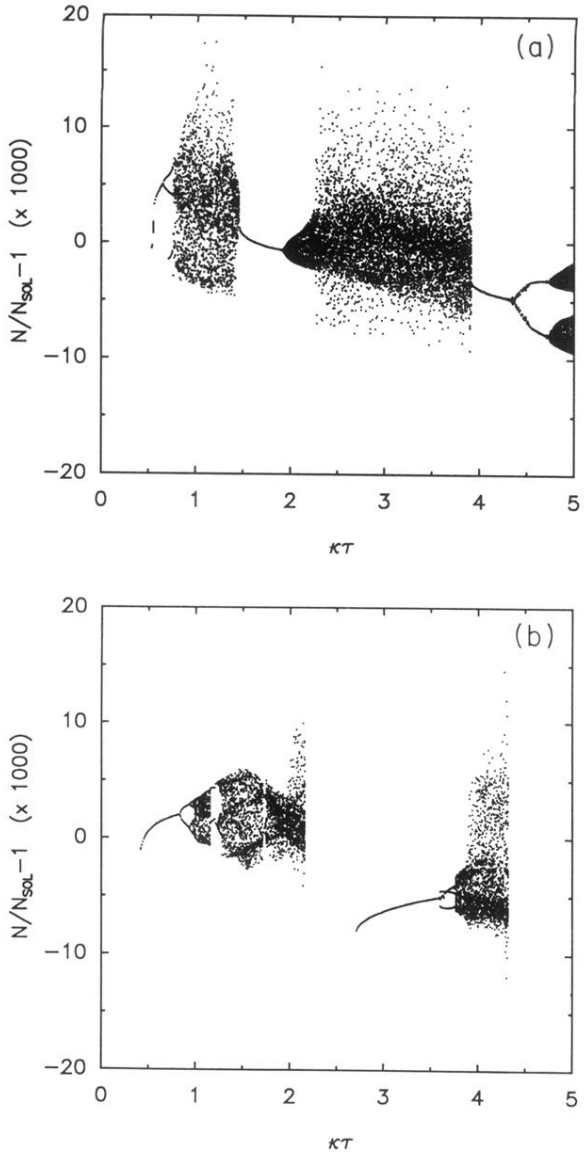

FIG. 1. Bifurcation diagrams in the cases of (a) PCF and (b) COF for $L_{ext}=10$ cm and $\alpha=3$. Other parameter values are shown in Table I. In the absence of feedback ($\kappa\tau=0$) the laser operates stably with 1.6 mW output power.

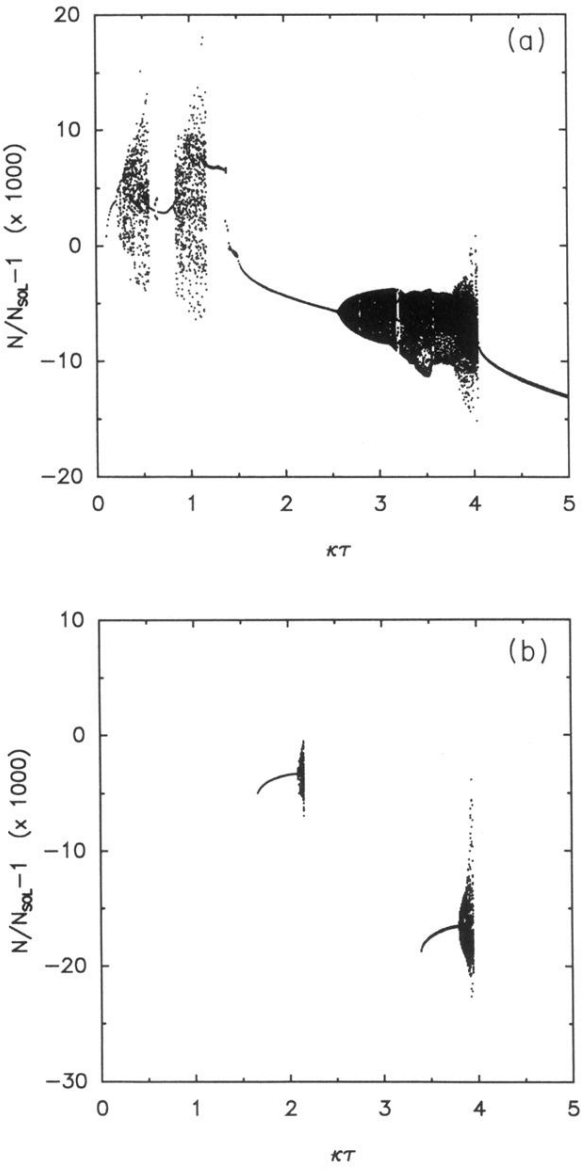

FIG. 2. Same as in Fig. 1 except that the external-cavity length L_{ext} has been reduced from 10 to 5 cm. The semiconductor laser is stable over a wide range of $\kappa\tau$ in the case of COF.

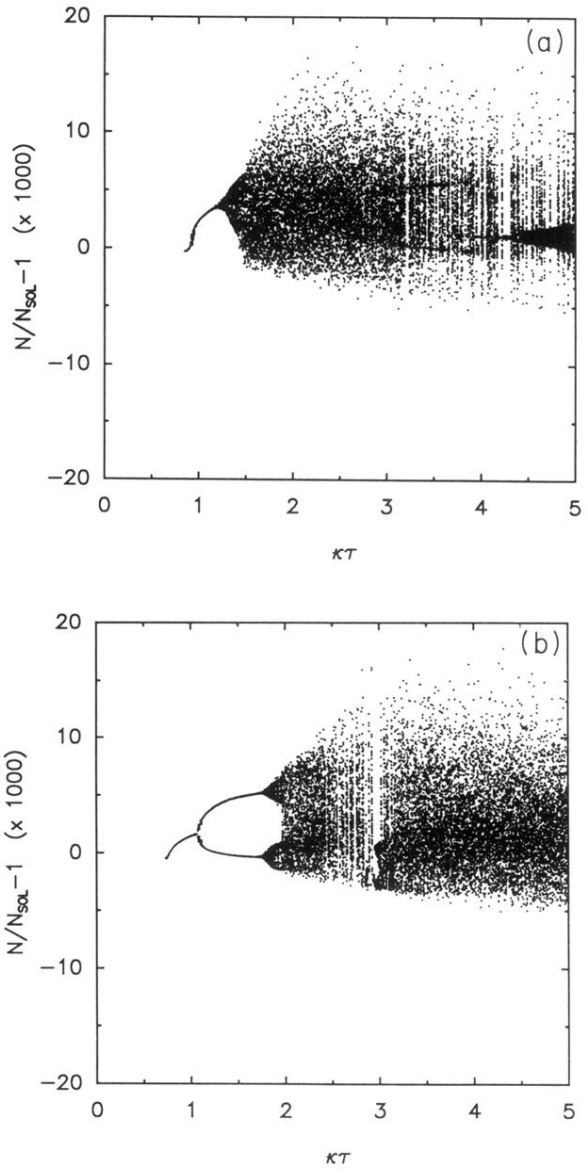

FIG. 3. Same as in Fig. 1 except that the external-cavity length L_{ext} has been increased to 30 cm. There are fewer differences between PCF and COF for longer external cavities.

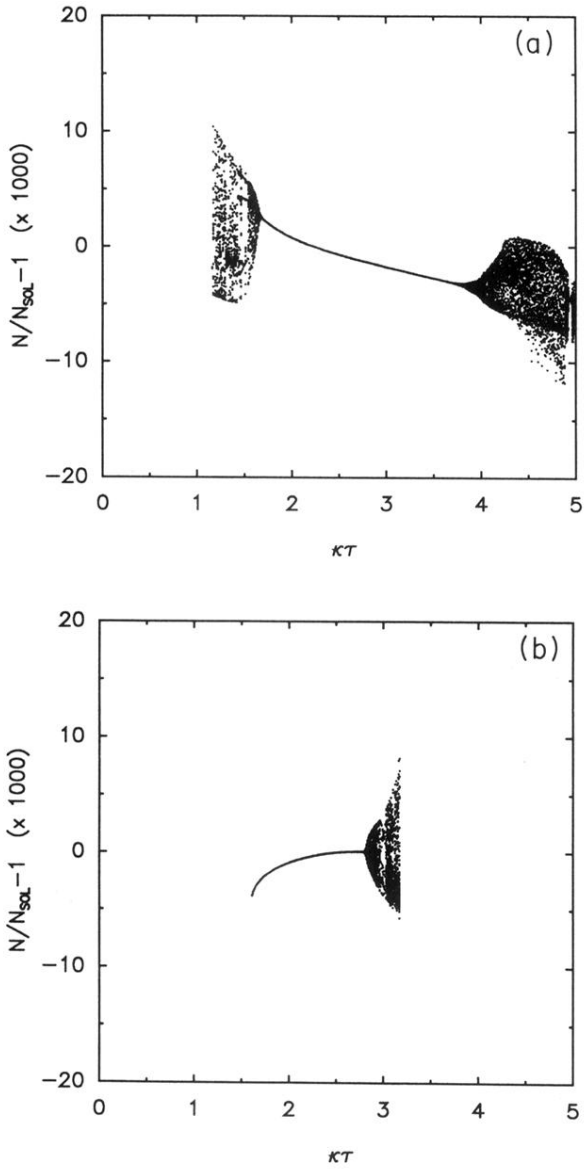

FIG. 4. Same as in Fig. 1 except that the linewidth enhancement factor α has been reduced from 3 to 1.5. The chaotic regions becomes sparser for smaller values of α in the cases of both PCF and COF. For PCF, the laser experiences an intermittency route to chaos (see Fig. 5).

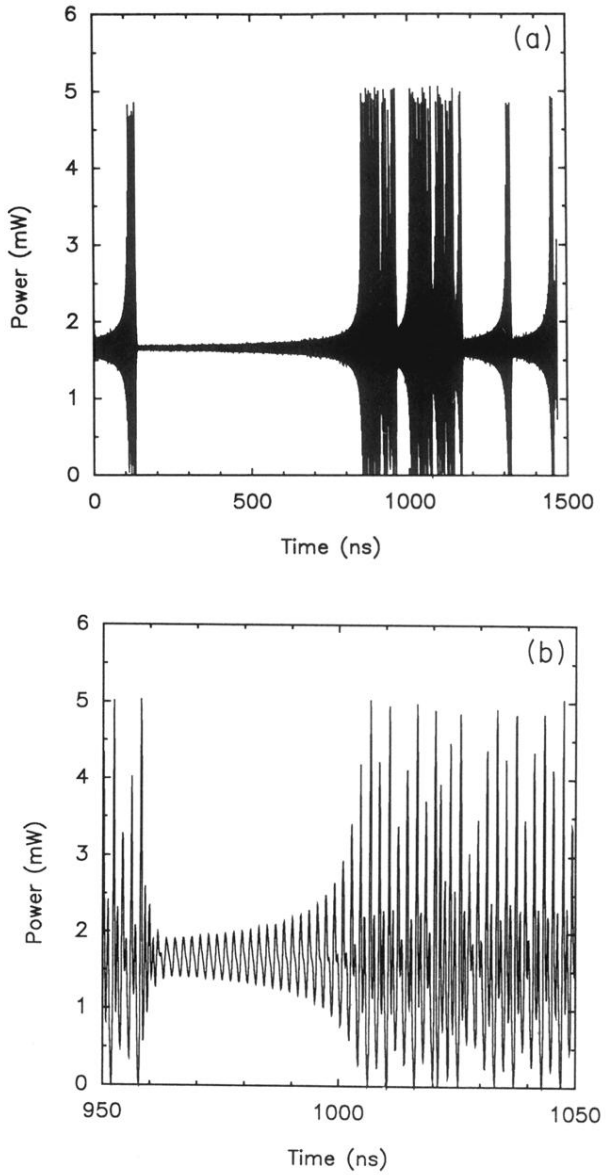

FIG. 5. (a) Long-time trajectory for PCF at $\kappa\tau = 1.3$ showing that the laser power undergoes intermittent bursts of chaotic output. (b) Blowup of a small region of (a) showing details of temporal evolution.

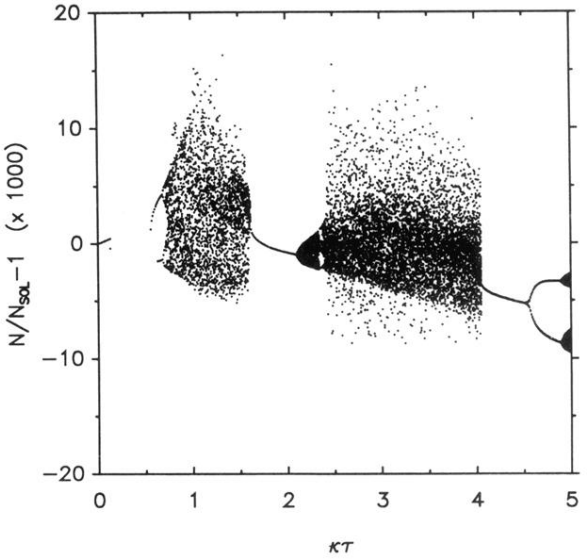

FIG. 9. Bifurcation diagram for PCF and 100 MHz detuning. Other parameters same as in Fig. 1. Note the presence of a periodic output for very small values of $\kappa\tau$ [compare with Fig. 1(a)] because of four-wave mixing.